ORIGINAL PAPER

M. Zhang · H. Xu · E. K. H. Salje · P. J. Heaney

Vibrational spectroscopy of beta-eucryptite (LiAlSiO$_4$): optical phonons and phase transition(s)

Abstract The structural behavior of β-eucryptite (LiAlSiO$_4$) has been investigated using infrared (IR) spectroscopy over a temperature range of 20 to 900 K and FT-Raman spectroscopy at room temperature. IR reflectance measurements show that β-eucryptite possesses high reflectivity in the far-IR region, as is consistent with its reported superionic conductivity along the c-axis. On heating, the Li-related IR bands near 246 and 300 cm^{-1} (with A_2 symmetry) broadened and weakened dramatically, presumably as a result of Li$^+$ positional disordering along the structural channels parallel to c. The disordering process appears to induce a framework distortion, as is evidenced by the broadening of some vibrations of Si(Al)–O with increasing temperature. A change in slope in the temperature dependence of the phonon frequency near 300 cm^{-1} and the linewidth of the 760 cm^{-1} band at $\sim$715 K indicates that Li becomes completely disordered above this temperature. In addition, the temperature dependence of the linewidth for the 760 cm^{-1} band exhibits an additional change in slope at 780 K, implying the existence of an intermediate state within this temperature range. The detailed structure of this intermediate phase, however, needs further study. Our IR data provide no indication of structural changes between room temperature and 20 K.

Keywords β-eucryptite · Infrared spectroscopy · Raman spectroscopy · Phase transition · Li disorder

M. Zhang (✉) · E. K. H. Salje
Department of Earth Sciences, University of Cambridge
Downing Street, Cambridge, CB2 3EQ, UK
e-mail: mz10001@esc.cam.ac.uk

H. Xu
Department of Chemical Engineering and Materials Science,
University of California at Davis, Davis,
California 95616, USA

P. J. Heaney
Department of Geosciences, Pennsylvania State University,
University Park, Pennsylvania 16802, USA

Introduction

Beta-eucryptite (LiAlSiO$_4$), a stuffed derivative of β-quartz, has attracted much interest due to its one-dimensional ionic conductivity and near-zero thermal expansion (Böhm 1975; Alpen et al. 1977; Nagel and Böhm 1982; Beall 1994). In β-eucryptite, Al and Si cations alternate in layers normal to the c-axis with concomitant positional ordering of Li ions within two distinct channels parallel to c (e.g., Buerger 1954; Schulz and Tscherry 1972a,b; Tscherry et al. 1972a,b; Pillars and Peacor 1973; Guth and Heger 1979). As a result, the translational periodicity of β-eucryptite is doubled along both c and a relative to the β-quartz structure, giving rise to the so-called c and a superlattice reflections in diffraction patterns of β-eucryptite. On heating, however, the so-called a superlattice reflections gradually disappear between 673 and 755 K; this behavior, which is reversible, is interpreted as evidence for positional disordering of the Li cations within the tunnels parallel to c at high temperatures (Tscherry and Laves 1970; Schulz and Tscherry 1972b; Pillars and Peacor 1973; Müller and Schulz 1976; Müller 1979). Based on their neutron scattering results, Press et al. (1980) argue that an intermediate incommensurate structure occurs over the temperature range from 703 to 763 K and that this phase coexists with the low-temperature structure from 703 to 755.5 K.

Despite the large number of studies that have focused on the Li disordering transformation in β-eucryptite, disagreements exist with respect to the following two issues. First, scientists have reported different degrees of variation in the intensities of the a-reflections (I) as a function of temperature. Consequently, the thermodynamic character of the transition has been described as first-order (Schulz and Tscherry 1972b), as second-order (Pillars and Peacor 1973), and as close to tricritical, with $\beta = 0.22$ in $I \sim (T_0 - T)^{2\beta}$ (Press et al. 1980). Second, although it is clear that Li$^+$ undergoes a positional disordering along the structural channels at

elevated temperatures (e.g., Tscherry et al. 1972a,b; Pillars and Peacor 1973), the role of the aluminosilicate framework in the transition is still a matter of debate. Schulz and Tscherry (1972b) argued that structural elements in the low-temperature phase are α-quartz-like, such that the framework changes its geometry in a manner that is analogous to the α-β-quartz transformation on heating. In addition, Press et al. (1980) interpreted the intermediate phase around the transition as an analogue to the incommensurate phase that occurs over a temperature interval of 1.3 K between α- and β-quartz (Dolino 1990). However, diffraction analysis using X-rays, neutrons and electrons indicated that β-eucryptite has a space group of $P6_222$ (or $P6_422$) (e.g., Tscherry et al. 1972a, b, Pillars and Peacor 1973, Müller 1979, Xu et al. 1999a), rather than $P3_221$ (or $P3_121$), as is the case for α-quartz. Moreover, a recent high-temperature transmission electron microscopy study of β-eucryptite did not reveal the Dauphiné twins that would be generated from a β-to-α quartz-like transformation (Xu et al. 1999b).

In light of the questions surrounding the transitions in β-eucryptite, we performed a series of infrared (IR) spectroscopic experiments from 20 to 900 K as well as FT-Raman measurements at room temperature. In situ IR spectroscopy has proved a powerful technique for studying phase transitions, because it can detect structural changes on a scale that is much more localized than is sampled by diffraction methods. Moreover, an analysis of the temperature evolution of the IR bands within different frequency regions allows us to determine the roles that the channel Li$^+$ cations and the aluminosilicate framework play in the structural transformation. Finally, the thermodynamic nature of the transitions can be ascertained with little ambiguity, since the order parameter is correlated with the phonon frequency and band width.

Sample synthesis and experimental methods

Samples

The β-eucryptite powder sample used in this study was synthesized from reagent-grade Li_2CO_3, Al_2O_3 and $SiO_2. \times HO_2$ chemicals. A mixture having a molar ratio of 1:1:2 with respect to these compounds was sintered in a Pt crucible in a Deltech vertical-tube furnace at about 1373 K for ~15 h. The resulting specimen was then ground and resintered at 1573 K for ~24 h. The final material consisted only of β-eucryptite, as revealed by powder X-ray diffraction (Xu et al. 1999a). In addition, a β-eucryptite single crystal (with a size of ~1.5 mm) was used for infrared reflectance and FT-Raman measurements. The crystal was grown from an LiF/AlF_3 flux. The detailed growth procedures have been described elsewhere (Schönherr and Schedler 1977).

IR spectroscopy

A conventional powder pellet technique (Zhang et al. 1996) was employed in this study. Sample pellets were prepared using KBr as a matrix material for the region of 500–1600 cm^{-1} and CsI for 180–700 cm^{-1}. All the IR spectra were recorded under vacuum with a Bruker 113v infrared spectrometer. A liquid-nitrogen-cooled MCT detector coupled with a KBr beamsplitter and a Globar source was used for the measurements in the mid-infrared (MIR) region, and a room-temperature DTGS detector coupled with 3.5-, 6-, and 23-μm Mylar beamsplitters and a Mercury source for the far-infrared (FIR) region. Instrumental resolution was set to 2 cm^{-1} coupled with a scan velocity of 6.25 KHz for FIR and 14.684 KHz for MIR. Each spectrum was calculated by Fourier transformation of 512 interferometer scans. For high-temperature measurements, the sample pellet was positioned within a cylindrical platinum-wound furnace using a recycled water-cooling system. The furnace was controlled with a Pt/PtRh thermocouple located close to the heating platinum wires in the furnace and a Eurothermal 815 temperature controller. The sample temperature was measured using an NiCr/NiAl thermocouple coupled with a Comark microprocessor thermometer. The NiCr/NiAl thermocouple was pressed against the sample and was calibrated against the α–β-quartz transition temperature. The temperature stability was better than 1 K. A closed-cycle liquid-nitrogen cryostat (LEYBOLD), equipped with a pair of KRS5 windows, was used for low-temperature experiments in the frequency range of 500–800 cm^{-1}. Room-temperature IR reflectance measurements were carried out on a small single crystal (~1.5 mm in size) in the frequency range of 20–5000 cm^{-1} using Au mirrors as the references (see Zhang and Salje 2001 for detailed information on the experimental setup). The experiments were performed under unpolarized conditions, because the crystal surfaces are not the ideal crystallographic planes needed for polarized measurements, and because cutting the crystal along the optimal planes would make the crystal too small to produce strong polarized signals in the FIR region using a DTGS detector.

Raman spectroscopy

The FT-Raman spectrum of β-eucryptite was recorded at room temperature using a Bruker IFS 66v spectrometer adapted with a Bruker FRA 106 FT-Raman accessory. An Nd = YAG laser with a wavelength of 1064 nm and a maximum output of 350 mW were used as the excitation source. A liquid-nitrogen-cooled high-sensitivity Ge detector was coupled with a silicon-coated calcium fluoride beamsplitter. The spectra were recorded with a laser power of 100 mW in a backscattering geometry. The resolution of all the spectra was 2 cm^{-1}. We noted that the spectral signals of powdered samples were not strong enough to reveal some weak bands. To detect these weak scattering lines and also to record the Raman modes with different symmetries, the small single crystal was measured at various crystal orientations and the data were then averaged to produce a final spectrum, which is essentially similar to that of powdered samples, but with a better signal-to-noise ratio.

Results and discussion

Room-temperature IR and Raman spectroscopy

As described earlier, β-eucryptite is an Li-stuffed derivative of β-quartz with the space group $P6_222$ or $P6_422$. For β-quartz, the irreducible representations of optical phonons can be given as: $1A_1 + 4E_2 + 4E_1 + 2A_2 + 3B_1 + 2B_2$ (Tezuka et al. 1991), where A_2 modes are IR-active, E_1 is both IR- and Raman-active, A_1 and E_2 are Raman-active, and B_1 and B_2 are optically silent. In β-eucryptite, however, since there are more atoms in the unit cell relative to β-quartz (the cell is doubled along both c and a due to the presence of Li), more vibrational modes are expected. An IR reflectance spectrum of β-eucryptite is shown in Fig. 1a. In order to extract the TO (transverse optical) and LO (longitudinal optical)
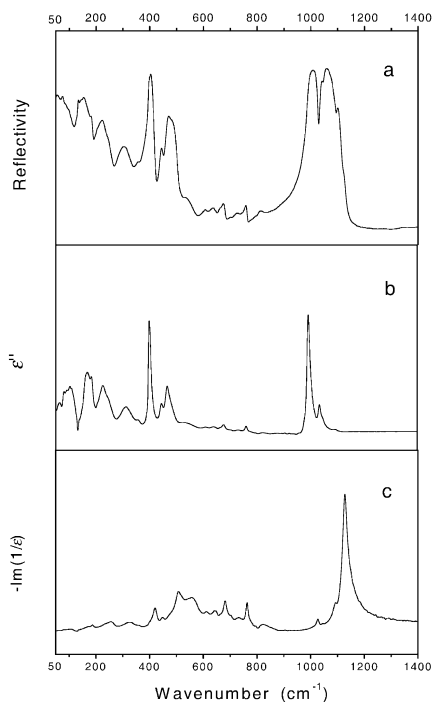
Fig. 1 a IR reflectance spectrum of β-eucryptite between 50 and 1400 cm^{-1}. **b** The imaginary part (ε'') of the dielectric constant. **c** The dielectric loss function, $-\mathrm{Im}(1/\varepsilon)$

Table 1 Observed IR modes of β-eucryptite and tentative mode assignments. ω_{TO} and ω_{LO} are the frequencies of transverse and longitudinal optical modes (in units of cm^{-1}), respectively

ω_{TO}	ω_{LO}	Symmetry	Assignment
1098	–[a]	E_1 (?)	Si–O stretching
1034	–	E_1	Si–O stretching
993	1129	A_2	Si/Al–O stretching
823	825	–	–
760	763	E_1	Si/Al–O stretching
736	737	–	?
677	684	A_2	Si/Al–O stretching
634 (?)	644	E_1	–
609	610	–	–
531	556	A_2	Si–O–Li bending
466	507	E_1	–
444	449	A_2	–
402	420	A_2	Si–O–Al vibration
355	359	E_1	–
300	326	A_2	Li–O stretching
246	255	A_2	Li–O stretching
225 (?)	232 (?)	A_2 (?)	–
183	186	E_1	–

[a] Not determined

phonons, the imaginary part (ε'') of the dielectric constant $[\varepsilon(\omega) = \varepsilon'(\omega) + i\varepsilon''(\omega)]$ and the dielectric loss function, $-\mathrm{Im}(1/\varepsilon) = \varepsilon''/(\varepsilon'^2 + \varepsilon''^2)$, were obtained through Kramers–Kronig analysis of the measured reflectance spectrum. The TO phonon frequencies (ω_{TO}) are given by peak positions in ε'', while LO phonon frequencies (ω_{TO}) can be obtained from the maximums of $-\mathrm{Im}(1/\varepsilon)$. The results of the analysis are shown in Fig. 1b and c, and the mode frequencies determined are listed in Table 1.

The infrared spectrum of β-eucryptiteis is characterized by strong absorption signals between 100 and 1400 cm^{-1} (Fig. 1a). Although assigning all the individual vibrational modes of β-eucryptite appears difficult or even impossible at this stage, the observed signals can be tentatively divided into three regions: (1) 700–1200 cm^{-1}; (2) 400–700 cm^{-1}; and (3) 100–400 cm^{-1}. The bands in the region 700–1200 cm^{-1} are mainly attributed to vibrations related to Si–O and Al–O stretching in the SiO$_4$ and AlO$_4$ tetrahedra (Moenke 1974; Zhang et al. 1996). The bands in the region 400–700 cm^{-1} have more complex natures. In β-eucryptite, the SiO$_4$ and AlO$_4$ tetrahedra are corner-linked to form channels along the c-axis. Si–O–Al linkages are formed, but direct Si–O–Si bridges are not favored, based on the Al avoidance principle (Loewenstein 1954, Goldsmith and Laves 1955). The stretching and bending of these Si–O–Al bridges are expected to appear in the in the 400–700 cm^{-1} region (Moenke 1974, McMillian 1984). In addition, vibrations of Si–O–Li bridges are known to exhibit bands in the range 500–600 cm^{-1} (Nocuñ and Handke

2001); these authors attribute a 531 cm^{-1} band to the bending of the Si–O–Li bridges because of its significant isotope effect. The bands between 100 and 400 cm^{-1} are mainly associated with Li ions and possible vibrations of T–O–T (T = Si or Al) as lithium silicates commonly show absorption associated directly with internal vibrations of LiO$_4$ tetrahedra between 250 and 460 cm^{-1}. Modes near 246 and 300 cm^{-1} are assigned as Li–O stretching as these bands showed isotope shifts of 8.7 and 10.6 cm^{-1}, respectively, through ^{6}Li/Li^7 isotope substitution (Nocuñ and Handke 2001).

One of the important features in the reflectance spectrum of β-eucryptite is the significant increase in reflectivity with decreasing wavenumber in the far-IR region. As is commonly seen in materials with high conductivities (such as high-T_c superconductors and metals, e.g., Yagil et al. 1995), this behavior suggests that β-eucryptite possesses high optical conductivity [optical conductivity $\sigma(\omega) = (\omega / 4)\,\mathrm{Im}(\varepsilon)$]. This behavior is consistent with its one-dimensional superionic conductivity reported in the literature (Alpen et al. 1977). Comparison of the IR with the Raman data (see later discussion) indicates that the Li-related bands near 246 and 300 cm^{-1} belong to the A_2 modes (Table 1). As the selection rules dictate that the resonances of A_2 symmetry occur when E, the electric vector of the incident infrared radiation, is parallel to the c axis, these Li–O stretching bands must vibrate along the c-axis. In other words, the motion of Li along the channels causes the observed high reflectivity or optical conductivity. In fact, the three mainly Li-related bands near 246, 300, and 531 cm^{-1} are all much broader than the bands associated with Si/Al–O vibrations. Moreover, they become broader with increasing temperature (see below). This behavior implies that Li indeed disorders along the channels on heating.
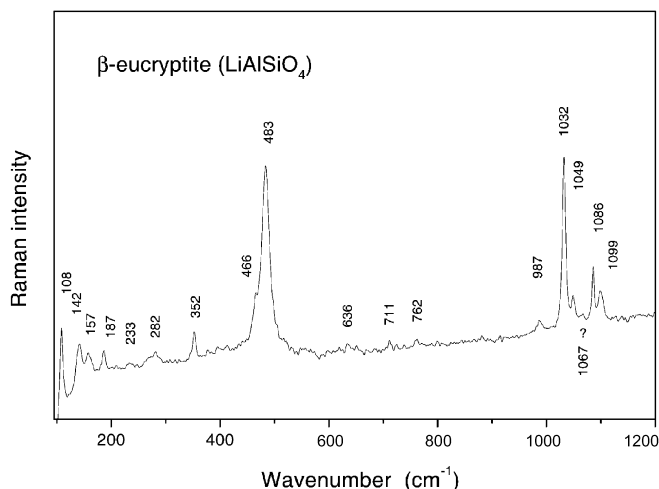
Fig. 2 FT-Raman spectrum of β-eucryptite in the region of 95–1200 cm^{-1}

FT-Raman spectra of β-eucryptite were recorded in order to help interpret the IR spectrum and to aid in the assignment of the E_1 and A_2 modes (E_1 modes are both IR- and Raman-active). The spectrum is shown in Fig. 2, where peak frequencies are also given. The Raman signals are characterized by two strong scattering lines near 484 and 1032 cm^{-1}. These two lines were assigned as A_1 modes by Sprengard et al. (2000). According to these authors, the former is a Si–O–Al symmetric stretching vibration caused by the oxygen motion along a line bisecting the Si–O–Al angle, whereas the latter is an antisymmetric stretching (Si–O–Al)
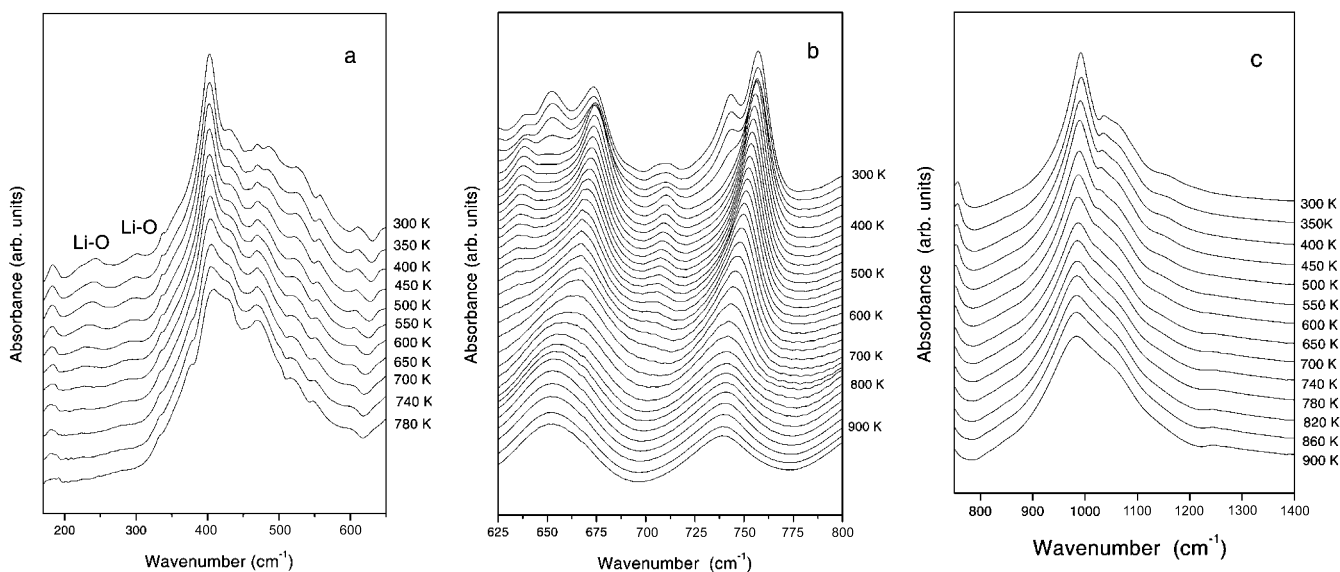
resulting from an in-phase movement of all four oxygen atoms relative to Si/Al at the tetrahedral center. In addition, there is a broad, weak Raman band near 282 cm^{-1}, and we assign it to the mode due to Li motions on the basis of its broad feature and low frequency.

Variable-temperature IR spectroscopy

The temperature evolution of the IR spectrum of β-eucryptite is shown in Fig. 3a–c. The effect of increasing temperature is generally seen as an increase in band width, a decrease in band intensity, and a shift in phonon frequency. For instance, the two IR bands (246 and 300 cm^{-1}) in the far-infrared region started to broaden at ~500 K and then showed dramatic decreases in intensity and increases in width upon further heating (Fig. 3a). In particular, the band near 246 cm^{-1} became essentially undetectable above ~710 K, while a new band appeared unexpectedly near 380 cm^{-1}. This behavior can be attributed to positional disordering of Li$^+$ along the structural channels parallel to c on heating, as was revealed by the previous diffraction studies (e.g., Tscherry et al. 1972a,b; Pillars and Peacor 1973; Müller 1979). Similar spectroscopic observations of thermally induced Li disorder have been reported in other Li-based compounds in nearly the same spectral regions (Teeters and Frech 1982; Zhang et al. 1998). Similarly, a recent IR study on the nonlinear optical material Li$_2$B$_4$O$_7$ (which also exhibits strong one-dimensional conductivity along the c axis at high temperatures) showed that bands in the FIR region undergo significant changes in response to Li disorder (Zhigadlo et al. 2001).

A thermally induced structural transition is typically manifested by a discontinuity in the temperature dependence of peak frequency or band width in the IR spectrum. As shown in Figs. 3a and 4, with increasing temperature, the frequency of the band at 300 cm^{-1}
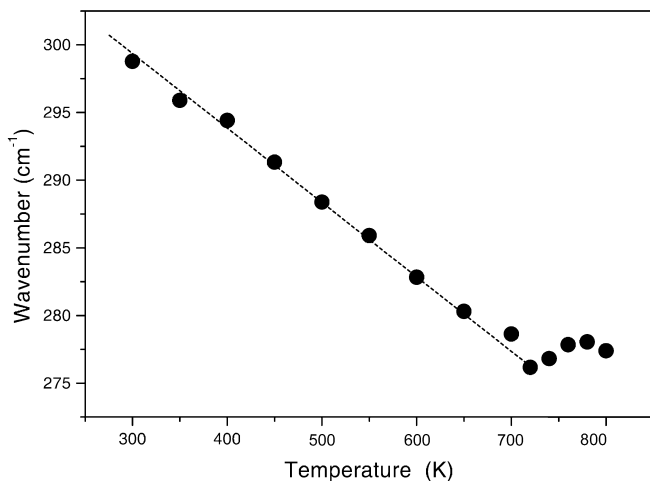
Fig. 3 The temperature evolution of powder infrared spectra of β-eucryptite. **a** In the region of 180–650 cm^{-1} between 300 and 780 K. **b** In the region of 625–800 cm^{-1} between 300 and 940 K (temperature interval = 20 K). **c** In the region of 750–1400 cm^{-1} between 300 and 900 K

Fig. 4 Variation of the peak position of the infrared band near 300 cm^{-1} as a function of temperature. The change in the temperature dependence of the band frequency ($\partial\omega/\partial T$) occurs near 715 K. *The line is a visual guide*

Fig. 5 Variation of linewidth Γ (FWHM) of the IR band near 760 cm^{-1} as a function of temperature. *The line is a visual guide*

decreases in a linear manner up to ~715 K and slightly increases thereafter, suggesting that the channel Li$^+$ ions become completely disordered at ~715 K. This T_c value is in general agreement with the previously published transition temperatures ranging from 673 to 755 K (Tscherry and Laves 1970; Schulz and Tscherry 1972b; Pillars and Peacor 1973; Müller and Schulz 1976; Müller 1979; Xu et al. 1999b). The large range of the reported T_c values is due not only to different synthesis conditions of the samples but also probably to variations in the resolution of the analytical techniques used. In the frequency range measured, we did not observe soft modes.

It appears that the order–disorder transition of Li$^+$ induces changes in the spectrum between 620 and 780 cm^{-1} (Fig. 3b). This frequency region generally contains the IR bands corresponding to T–O modes and has been chosen for studying displacive transitions in quartz (Salje et al. 1992) and tridymite (Cellai et al. 1995). With increasing temperature, the bands at 673 cm^{-1} and 760 cm^{-1} soften in frequency and broaden in width. Moreover, with increasing temperature, the linewidth (full width at half maximum, FWHM) of the 760 cm^{-1} band shows a much steeper increase (about 50%) between 715 and 780 K (Figs. 3a, 5). The complex variation in the features of these IR bands implies that the aluminosilicate framework may distort in response to the Li positional disordering on heating. As described by Palmer (1994), the occupancy of Li$^+$ ions in the tetrahedral channel sites tends to shorten the O–O edges that are shared by the Li- and Si(Al)-tetrahedra to minimize the Li–Si(Al) repulsion. As a result, the positional disordering of Li on heating can induce corresponding geometrical changes in the framework through Si(Al)-tetrahedral deformation and tilting (Xu et al. 1999a). Nevertheless, the framework distortion is a rather gradual and complex process, and it does not behave like
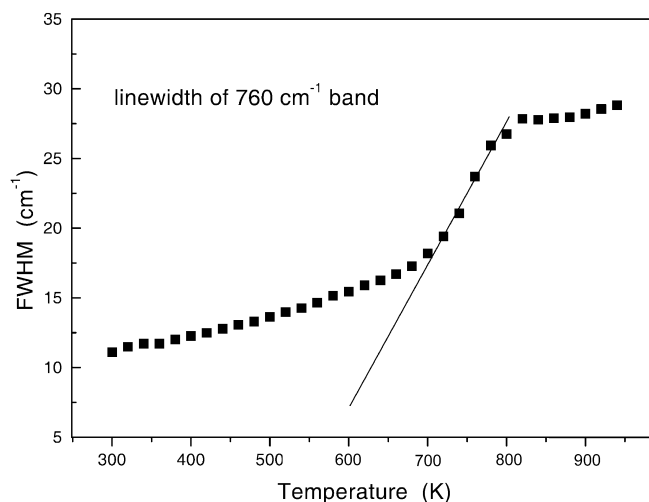
the α–β quartz transformation, that would produce Dauphiné microtwins at the transition (Xu et al. 1999b).

In contrast to the relatively strong temperature dependence of phonon bands at 246, 300, 677 and 993 cm^{-1}, the IR bands between 400 and 600 cm^{-1} appeared to change only slightly in frequency with increasing temperature (The band at 402 cm^{-1} is an exception, as it showed a small hardening above 700 K). The bands over this region of the spectrum are due mainly to Si–O–Al bending. Apart from in situ high-T measurements, powder absorption experiments were also carried out at low temperatures. On cooling to 20 K, the IR spectra between 500 and 800 cm^{-1} remained virtually unchanged, except for a slight sharpening. This behavior suggests that no phase transition in β-eucryptite occurs below room temperature.

Although the temperature dependence of the phonon frequency at 300 cm^{-1} or the linewidth (Γ) of the band near 760 cm^{-1} suggests a singular transition at ~715 K (Fig. 3a and b), the plot of the linewidth (Γ) of the 760 cm^{-1} band as a function of temperature (Fig. 5) shows two changes in slope at 720 and 780 K. This behavior might be correlated with the two transitions involving the intermediate phase that exists between 703 and 763 K, as revealed by neutron scattering (Press et al. 1980). However, the formation mechanism of this intermediate structure, especially the probable interaction between the channel Li and aluminosilicate framework at the transition, merits further study. In addition, we note that the bands at 652 cm^{-1} and 743 cm^{-1} (frequencies from powder samples) show a dramatic decrease in intensity when the temperature is increased to ~380 K (Fig. 3b). This spectral anomaly cannot possibly result from the removal of H$_2$O on heating, because no water bands are seen near 1600 cm^{-1} at all temperatures. The change could be associated with the onset of significant Li mobility. Experiments are desirable to clarify this issue.

References

Alpen UV, Schulz H, Talat GH, Böhm H (1977) One-dimensional cooperative Li-diffusion in β-eucryptite. Solid State Commun 23: 911–914

Beall GH (1994) Industrial applications of silica. In: Heaney PJ, Prewitt CT, Gibbs GV (eds) Silica. Reviews in mineralogy, vol 29. Mineralogical Society of America, Washington DC, pp 468–505

Böhm H, (1975) Dielectric properties of β eucryptite. Phys, Status Solidi A 30: 581–536

Buerger MJ (1954) The stuffed derivatives of the silica structures. Am Mineral 39: 600–614

Cellai D, Carpenter MA, Kirkpatrick RJ, Salje EKH, Zhang M (1995) Thermally induced phase transitions in tridymite: an infrared spectroscopy study. Phys Chem of Miner 22: 50–60

Dolino G (1990) The α-inc-β transition of quartz: a century of research on displacive phase transitions. Phase Transitions 21: 59–72

Goldsmith JR, Laves F (1955) Cation order in anorthite (CaAl$_2$Si$_2$O$_8$) as revealed by gallium and germanium substitutions. Z Kristallog 106: 213–226

Guth H, Heger G (1979) Temperature dependence of the crystal structure of the one-dimensional Li$^+$-conductor β-eucryptite (LiAlSiO$_4$). In: Vashita P, Mundy JN and Shenoy GK (eds) Fast ion transport in solids. Elsevier, New York, pp 499–502

Loewenstein W (1954) The distribution of aluminum in the tetrahedra of silicates and aluminates. Am Mineral 39: 92–96

Moenke HHW (1974) Silica, the three-dimensional silicates, brosilicates and beryllium silicates. In: Farmer VC (ed) The infrared spectra of minerals, Mineralogical Society, London, pp 365–381

McMillian P (1984) Structural studies of silicates glasses and melts – applications and limitations of Raman spectroscopy. Am Mineral 69: 622–644.

Müller WF (1979) The effect of heating on the domain structure of beta-eucryptite, LiAlSiO$_4$. J Mater Sci 14: 1433–1439

Müller WF, Schulz H (1976) Antiphase domains in β-eucryptite (LiAlSiO$_4$). Naturwissenschaften 63: 294

Nagel W, Böhm H (1982) Ionic conductivity studies on LiAlSiO$_4$–SiO$_2$ solid solutions of the high quartz type. Solid State Commun 42: 625–631

Nocuň M, Handke M (2001) Identification of Li-O absorption bands on lithium istope substitutions. J Molec Struct 596: 145–149

Palmer DC (1994) Stuffed derivatives of the silica polymorph. In Heaney PJ, Prewitt CT, Gibbs GV (eds) Silica. Reviews in mineralogy, vol 29. Mineralogical Society of America, Washington DC, pp 83–122

Pillars WW, Peacor DR (1973) The crystal structure of beta eucryptite as a function of temperature. Am Mineral 58: 681–690

Press W, Renker B, Schulz H, Böhm H (1980) Neutron scattering study of the one-dimensional ionic conductor β eucryptite. Physical Review (B) 21: 1250–1257

Salje EKH, Ridgwell A, Güttler B, Wruck,B, Dove MT, Dolino G (1992) On the displacive character of the phase transition in quartz: a hard-mode spectroscopy study. J Phys Condens Matter 4: 571–577

Schönherr E, Schedler E (1977) The growth of β-LiAlSiO$_4$ crystals from high temperature solution in LiF–AlF$_3$ mixtures. J Crystal Growth 42: 289–292

Schulz H, Tscherry V (1972a) Structural relations between the low- and high-temperature forms of β-eucrypite (LiAlSiO$_4$) and low and high quartz. I. Low-temperature form of β-eucrypite and low quartz. Acta Crystallogr (B) 28: 2168–2173

Schulz H, Tscherry V (1972b) Structural relations between the low- and high-temperature forms of β-eucrypite (LiAlSiO$_4$) and low and high quartz. II. High-temperature form of β-eucrypite and high quartz. Acta Crystallogr (B) 28: 2174–2177

Sprengard R, Binder K, Brändle M, Fotheringham U, Sauer J, Pannhorst W (2000) On the interpretation of the experimental Raman spectrum of β-eucryptite LiAlSiO$_4$ from atomistic computer modelling. J Non-Crystal Solids 274: 264–270

Teeters D, Frech R (1982) Temperature dependence of the Raman-active lithium modes in LiKSO$_4$ and LiNaSO$_4$. Phys Rev (B) 26: 4132–4139

Tezuka Y, Shin S, Ishigame M (1991) Observation of the silent phonon in β-quartz by means of hyper-Raman scattering. Phys Rev Lett 66: 2356–2359

Tscherry V, Laves F (1970) Synthesis and X-ray reflection pattern of β-eucryptite. Naturwissenschaften 57: 194

Tscherry V, Schulz H, Laves F (1972a) Average and super structure of β eucryptite (LiAlSiO$_4$), part I. Average structure. Z Kristallogr 135: 161–174

Tscherry V, Schulz H, Laves F (1972b) Average and super structure of β eucryptite (LiAlSiO$_4$). part II. Superstructure. Z Kristallogr 135: 175–198

Xu H, Heaney PJ, Yates DM, Von Dreele RB, Bourke MA (1999a) Structural mechanisms underlying near-zero thermal expansion in β-eucryptite: a combined synchrotron X-ray and neutron Rietveld analysis. J Mater Res 14: 3138–3151

Xu H, Heaney PJ, Böhm H (1999b) Structural modulations and phase transitions in β-eucryptite: an in-situ TEM study. Phys Chem Miner 26: 633–643

Yagil Y, Baudenbacher F, Zhang M, Birch JR, Kinder H, Salje EKH (1995) Phys. Rev (B) 52: 15582–15591

Zhang M, Salje EKH (2001) Infrared spectroscopic analysis of zircon: radiation damage and the metamict state. J Phys Condens Matter 13: 3057–3071

Zhang M, Wruck B, Graeme-Barbar A, Salje EKH, Carpenter MA (1996) Phonon-spectroscopy on alkali-feldspars: phase transitions and solid solutions. Am Mineral 81: 92–104

Zhang M, Salje EKH, Putnis A (1998) Phase transitions in LiKSO$_4$ between 1.5 K and 850 K: an infrared spectroscopic study. Journal of Physics: Condensed Matter 10: 11811–11827

Zhigadlo ND, Zhang M, Salje EKH (2001) An infrared spectroscopic study of Li$_2$B$_4$O$_7$. J Phys Condens Matter 13: 6551–6561